4. R. E. Walstedt, W. W. Warren, Jr., R. F. Bell, G. F. Brennert, J. P. Remeika, R. J. Cava, and E. A. Rietman, *Phys. Rev.*, **B36,** 5727 (1987).
5. M. A. Beno, L. Soderholm, D. W. Capone II, D. G. Hinks, J. D. Jorgensen, I. K. Schuller, C. U. Segre, K. Zhang, and J. D. Grace, *Appl. Phys. Lett.*, **50,** 543 (1987).
6. C. H. Pennington, D. J. Durnand, D. B. Zax, C. P. Slichter, J. P. Rice, and D. M. Ginsberg, *Phys. Rev.*, **B37,** 7944 (1988).
7. T. Shimizu, H. Yasuoka, T. Imai, T. Tsuda, T. Takabatake, Y. Nakazawa, and M. Ishikawa, *J. Phys. Soc. Jpn.*, **57,** 2494 (1988).
8. H. So and R. L. Belford, *J. Am. Chem. Soc.*, **91,** 2392 (1969); H. So, Ph. D. Thesis, University of Illinois at U.-C., 1970.
9. R. M. Sternheimer, *Phys. Rev.*, **164,** 10 (1967).
10. A. J. Freeman and R. E. Watson in "Magnetism," G. T. Rado and H. Suhl, Eds., Vol. IIA, Academic Press, New York, N. Y., p. 291, 1965.
11. F. A. Cotton, C. B. Harris, and J. J. Wise, *Inorg. Chem.*, **6,** 909 (1967).
12. S. Horn, J. Cai, S. A. Shaheen, Y. Jeon, M. Croft, C. L. Chang, and M. L. denBoer, *Phys. Rev.*, **B36,** 3895 (1987).
13. J. A. Yarmoff, D. R. Clarke, W. Drube, U. O. Karlsson, A. Taleb-Ibrahimi, and F. J. Himpsel, *Phys. Rev.*, **B36,** 3967 (1987).
14. T. A. Sasaki, Y. Baba, N. Masaki, and I. Takano, *Jpn. J. App. Phys.*, **26,** L1596 (1987).
15. S. Horn, J. Cai, S. A. Shaheen, M. Croft, C. L. Chang, and M .L. denBoer, *J. Appl. Phys.*, **63,** 4193 (1988).
16. D. H. Kim, D. D. Berkeley, A. M. Goldman, R. K. Schulze, and M. L. Mecartney, *Phys. Rev.*, **B37,** 9745 (1988).
17. A. J. Freeman, J. Yu, S. Massiada, C. L. Fu, and J. H. Xu, *J. Appl. Phys.*, **63,** 4220 (1988).
18. M. H. Whangbo, M. Evain, M. A. Beno, J. M. Williams, *Inorg. Chem.*, **26,** 1831 (1987).
19. R. E. Watson and A. J. Freeman, *Phys. Rev.*, **131,** 250 (1963).
20. J. J. Bour, P. J. M. W. L. Bieker, and J. J. Steggerda, *Inorg. Chem.*, **10,** 1202 (1971).
21. P. J. M. W. L. Birker, *Inorg. Chem.*, **16,** 2478 (1977).
22. For example, see G. F. Holland, and A. M. Stacy, *Acc. Chem. Res.*, **21,** 8 (1988).

The Structural Features and Rotational Barriers in Indenyl Allyl Metal Complexes

Sungkwon Kang

Department of Chemistry, Chungnam National University, Taejeon 305 – 764. *Received August 31, 1989.*

The electronic structure, conformational preferences, and rotational barriers have been studied for transition metal indenyl allyl complexes by means of extended Hückel calculations. After geometrical optimization the exo conformation of allyl moiety is favored over the endo. The rotational barrier of indenyl ring in (Indenyl)Mo(CO)$_2$(Allyl) is computed to be 3.8 kcal/mol. Population analysis is applied to account for the conformational preferences and rotational barriers. A series of substituted allyl complexes has been also optimized. It shows steric hindrance plays a crucial role in setting the allyl orientation.

Introduction

There is interest in the conformational preferences and rotational barriers in polyene transition metal complexes. It is a common field which has been investigated by theoreticians and experimentalist. There are many experimental data on rotational barriers of organometallic compounds, as well as on conformational preferences studied mainly by NMR technique and diffraction methods.[1] Recently several studies have been reported on the polyene allyl complexes which show a variety of reactivity and interesting stereospecificity on the allyl group. The crystal structures of ML_n(allyl)(polyene), polyene = cyclopentadienyl(Cp) or indenyl(In), show exo orientation (1) of allyl group.[2] However, these complexes exhibit exo-endo (2) interconversion. This paper describes the electronic structure of transition metal indenyl dicarbonyl allyl complexes with an emphasis on conformational preferences and rotational barriers. We have also examined a series of substituted allyl complexes to determine the orientation of the allyl moiety. There are two kinds of rotational barrier in indenyl allyl complexes. Those are concerned with indenyl and allyl units. We shall first concentrate our attention on the electronic and geometrical requirements for the allyl moiety. But before we do so, it is necessary to investigate the metal fragment orbitals. Our computations are of the extended Hückel method with details given in the Appendix.

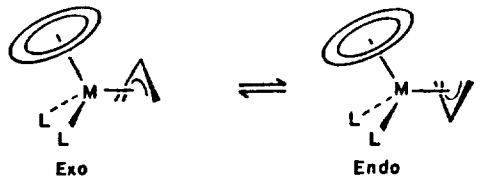

1 2

The (Indenyl)M(CO)$_2$ Fragment. The orbitals of (In)M(CO)$_2$ fragment is very similar to that of CpM (CO)$_2$ fragment which can be obtained in a number of ways.[3,4] We shall briefly describe the salient features of the analysis. The

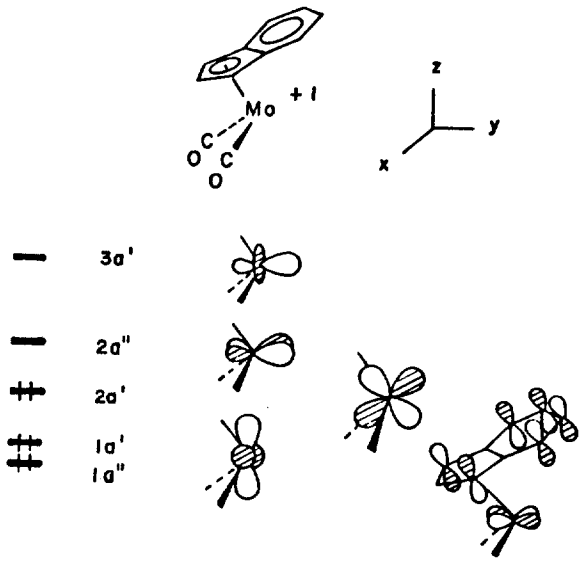

Figure 1. The valence orbitals of a d^4-(Indenyl)Mo$(CO)_2^+$ fragment.

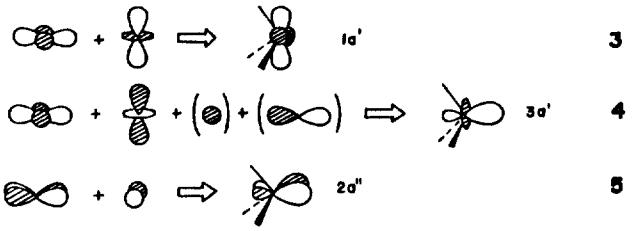

valence orbitals of a d^4-(In)Mo$(CO)_2^+$ are shown in Figure 1. With the given coordinate system, the 2a orbital is predominantly *yz* of metal. The x^2-y^2 and z^2 metal d orbitals intermix a little to give same symmetry fragment orbitals, 1a'(3) and 3a'. The 3a' orbital becomes hybridized by further mixing some *s* and *y* character. The resultant orbital, 4, is hybridized toward the missing ligand. The 2a" orbital is also perturbed by metal *x* from *xy* shown in 5. The hybridized 2a" and 3a' orbitals are empty for a d^4 fragment. And these orbitals obviously play an important role when real molecules are formed from this fragment. At the lower level the 1a" orbital is mainly indenyl π-orbital and small portion of metal. In the *Cp* ligand, this 1a" type fragment orbital lies much lower energy and is not involved in the interaction with the other valence orbitals. With the indenyl ligand, however, the energy of 1a" orbital is close to the other metal *d* orbitals because of the π orbital in indenyl ligand.

(Allyl)Mo$(CO)_2$(Indenyl) complexes. We investigate molecular orbitals of the exo and endo structures of (Allyl)Mo$(CO)_2$(In) to study the reason behind the conformational preference. We optimized structures at the two extreme orientations of allyl moiety. Two angle variables α and β (defined in 6) were used for the optimization of allyl geometry. The

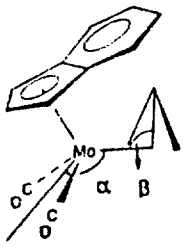

6

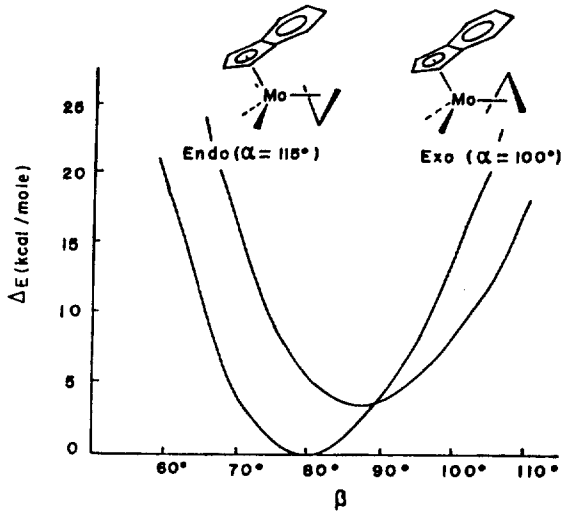

Figure 2. The energy profile for the exo ($\alpha = 100°$) and endo ($\alpha = 115°$) conformations of (Allyl)Mo$(CO)_2$(Indenyl) as a function of β.

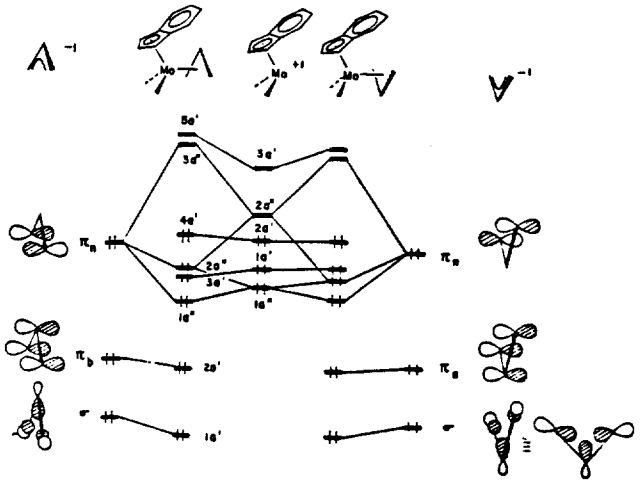

Figure 3. Interaction diagrams for the Exo(1) and Endo(2) conformations in (Allyl)Mo$(CO)_2$(Indenyl) complex.

angle β is related to the distance between metal and center carbon of allyl unit. We find that the optimum structures of (Allyl)Mo$(CO)_2$(In) as a function of the above two variables are $\alpha = 100°$, $\beta = 81°$ for the exo and $\alpha = 115°$, $\beta = 87°$ for the endo conformer. We do not expect the extended Hückel method to give us perfect structure. When the β value is 90.13°, all three distances between metal and three carbons in allyl unit are identical. The optimum geometry in exo shows that the distance between metal and center carbon is shorter than the other two that was observed in X-ray crystal structure of Cp or (In)-Mo$(CO)_2$(Allyl).[2a,d] Furthermore, the exo conformer is favored over the endo in total energy. Figure 2 shows total energy profile of the exo ($\alpha = 100°$ fixed) and endo ($\alpha = 115°$) as a function of β. The curves are well balanced in energy for the two extreme allyl orientations and the calculated difference in energy between the two is favoring the exo conformer by 3.7 kcal/mol. The crystal structure of Mo complex has the exo orientation.[2a]

The electronic structures of the endo conformer of (Allyl)M$(CO)_2$(Cp) complex has been briefly discussed by Schilling and Hoffmann in the context of CpMLL'(allyl) and

-(ethylene) complexes.[5] We here discuss the indenyl system with the available crystal structures. Figure 3 shows the interaction diagram for allyl^{-1} and Mo(CO)$_2$(In)$^{+1}$ fragments in the exo and endo conformers. In the center of Figure 3 are the five valence orbitals of metal fragment previously discussed. At the far left and right of Figure are two π and one σ orbitals of allyl fragment. There are three important π-type orbitals in allyl ligand. These are labeled as a bonding π_b, a nonbonding π_n, and an antibonding π_a. Only two lower energy orbitals are shown in Figure 3. At lower energy is σ orbital which is carbon-carbon σ bonding in allyl ligand. At the exo conformer (left side of Figure 3) 2a′ of metal fragment remains nonbonding to produce highest occupied molecular orbital (HOMO), 4a′ in complex. The 1a′ metal fragment orbital is a little stabilized by the π_a (not shown in Figure) in allyl unit. The 1a″ and 2a″ combinations of metal fragment overlap with π_n to form a three orbital pattern. The 1a″ molecular orbital (7) is bonding interaction between above two metal fragmental orbitals and π_n. At the higher energy metal fragment 1a″ interacts with π_n in an antibonding fashion; however, metal fragment 2a″ enters in a bonding way with respect to π_n of the allyl fragment to form 2a″ molecular orbital. The component of 2a″ M.O. is 40% 1a″, 32% 2a″, and 21% π_n. At much higher energy 1a″ and 2a″ both interact with π_n in an antibonding fashion to produce 3a″(8). In (In)Mo(CO)$_2$(Allyl) this becomes the lowest

7 8

unoccupied molecular orbital. In the case of cyclopentadienyl for polyene, this orbital is concentrated on the terminal carbons of the allyl ligand[5] and could play an important role when a nucleophile attacks the allyl ligand.[6] Two lower molecular orbitals (1a″ and 2a″) in three orbital interaction are occupied by four electrons. These interactions are primary driving force to stabilize (Allyl)Mo(CO)$_2$(In) complex. The molecular levels 1a′ and 2a′ are primarily allyl σ and π_b, respectively, a little mixed in a bonding way with metal 3a′.

The electronic structure of the endo conformer (shown in the right side of Figure 3) is very similar to that of the exo. There is nothing to further describe the interaction diagram of the endo. What is more interesting point is the energy difference between the exo and the endo conformers. We already described the exo is favorable over the endo conformer by 3.7 kcal/mol. One way to quantify this manner is via the Mulliken overlap population analysis.[7] As discussed in metal fragment orbitals, metal 2a″ is hybridized toward the empty coordinate site. Therefore, the metal 2a″ interacts more strongly than the metal 1a″ with allyl π_n. The overlap population coming from 2a″-π_n interaction (see Figure 3) for the exo is 0.1833 and 0.1796 for the endo. According to the bigger overlap value of the exo we can easily expect that the exo is the preferred conformer. We calculated the stabilization energy rising from this interaction. The stabilization energy in 2a″-π_n interaction is 47.9 kcal/mol for the exo and 45.7 kcal/mol for the endo. The difference is 2.2 kcal/mol. This is

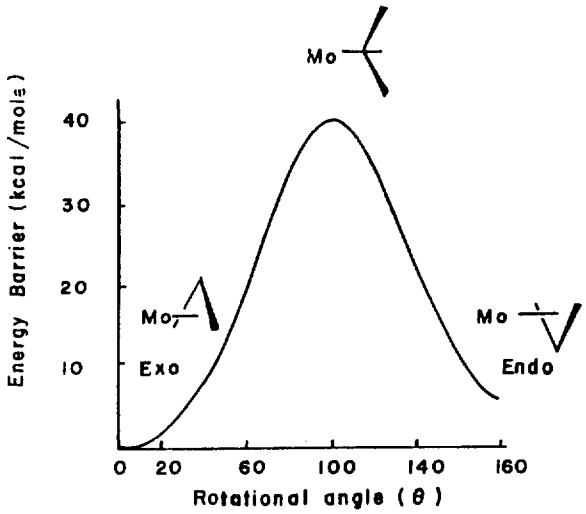

Figure 4. The rotational barrier of allyl unit in (Allyl)Mo(CO)$_2$(Indenyl) as a function of θ.

about 60% of the total energy difference between the exo and the endo conformers. The remaining energy difference is spread all over the other interactions shown in Figure 3.

Rotational Barriers in Mo complex. The activation energy of the exo and endo interconversion in (Allyl)M(CO)$_2$(polyene), M = Mo or W, has been measured as 14-17 kcal/mol.[8,9] When the simple rotational pathway (9) has been chosen for the M = Mo and polyene = Indenyl, the computed

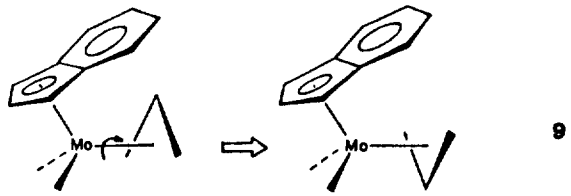

9

barrier, 40.4 kcal/mol (shown in Figure 4), is more than twice of the observed. As R. Hoffmann already pointed out,[5] the large activation barrier comes for the loss of 2a″-π_n interaction (see Figure 3) when the allyl unit is rotated by about 100°. Obviously 9 is not a reasonable pathway for exo-endo interconversion. Other possible mechanism is π-σ-π pathway.[10] In other words, η^3-allyl group (π-type) changes to η^1(σ-type) followed by rotation around the new C-C single bond, and then collapse back to the η^3-allyl group. However, we will not discuss this mechanism anymore in this paper.

The rotational barrier of polyene ligand in (polyene)ML$_n$ system shows large range depending on the types of polyene and metal fragment. This is from >1 kcal/mol to 20 kcal/mol.[11] A lot of investigations have been reported about the rotation in cyclopentadienyl and arene complexes.[12] Also molecular orbital calculations have appeared which explain the rotational barriers observed.[11,13] However, little work has been reported of barrier to indenyl rotation about a ring-metal axis.[14] It has been known that the rotational barrier of indenyl is larger than that of cyclopentadienyl group. Our extended Hückel calculations give a barrier of 1.0 kcal/mol for the Cp ring in (Cp)Mo(CO)$_2$(Allyl) complex. And 3.8 kcal/mol for the indenyl ring has been computed in indenyl analog.

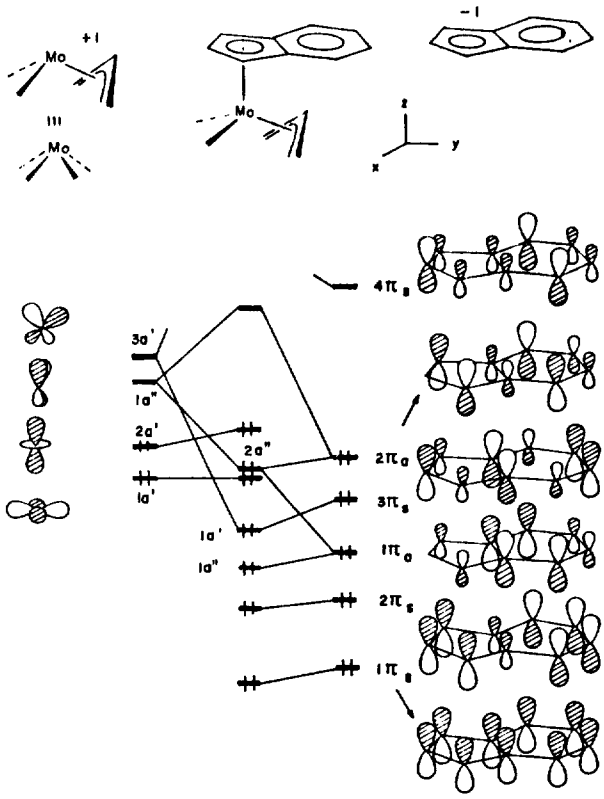

Figure 5. An orbital interaction diagram for (In)Mo(CO)$_2$(Allyl) with Indenyl^{-1} and Mo(CO)$_2$(Allyl)$^{+1}$ fragments.

Consider the interaction diagram given in Figure 5 where the geometry is taken from the previously optimized structure. At Figure 5 we used different fragments compared with Figure 3 to focus the indenyl rotation. But molecular orbital levels (center of Figures) should be same in energy. At the metal fragment, Mo(CO)$_2$(Allyl)$^+$, allyl ligand can be considered four electrons donor anionic ligand. Then this fragment is isolobal[15] with Mo(CO)$_4^{+2}$ unit. The orbitals of C_{4v} ML$_4$ fragment have been extensively discussed elsewhere,[16] and we will only point out the salient features. The left side of Figure 5 shows four metal centered orbitals in Mo(CO)$_2$(Allyl)$^+$. Two lower orbitals, 1a′ and 2a′, are primarily metal x^2-y^2 and z^2. At higher energy are 1a″ and 3a′ metal xz and yz perturbed by metal x and y, respectively (10 and 11). The resulting fragment orbitals are hybridized toward the miss-

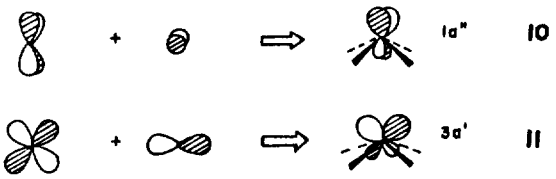

ing coordinate site. We can easily see these two hybridized orbitals strongly overlap with the indenyl orbitals. Only the important π orbitals of indenyl are shown on the right of Figure 5. Here we have labeled them with a subscript which refers to their symmetry with respect to the mirror plane. 1a′ and 2a′ of metal fragment are largely nonbonding. The empty 1a″ and 3a′ set of metal stabilizes $1\pi_a$, $3\pi_s$, and $2\pi_a$. These combinations contain by far the most significant interactions

Table 1. The Optimized Geometries and Relative Energies for (Allyl)Mo(CO)$_2$(Indenyl) in the two Extreme Orientations of Substituted Allyl Units. α and β are defined in 6

Allyl	Exo	Endo	ΔE^a(kcal/mole)
1-s-Me	$\alpha=100, \beta=81$	$\alpha=115, \beta=87$	3.7
1-a-Me	$\alpha=100, \beta=82$	$\alpha=115, \beta=88$	3.8
1,1-Me$_2$	$\alpha=110, \beta=78$	$\alpha=110, \beta=82$	9.7
2-Me	$\alpha=110, \beta=79$	$\alpha=110, \beta=84$	11.6
	$\alpha=90, \beta=92$	$\alpha=115, \beta=93$	-17.6

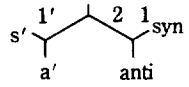

in the complexation of Mo(CO)$_2$(Allyl)$^+$ to indenyl ligand. There is a three orbital interaction pattern. At the middle the molecular 2a″ orbital is primarily given by 1a″ metal fragment orbital with $2\pi_a$ mixed into it in bonding fashion. Additionally some $1\pi_a$ character mixes in with the phase relationship shown in 12 (antibonding to 1a″). The drawing is

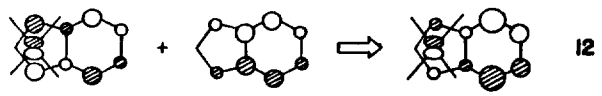

given in top view. Most of electron density for π-type is localized in the uncoordinated benzene ring. As we have mentioned previously the rotational barrier of indenyl unit is 3.8 kcal/mol. This barrier obtains at the 126° rotation of indenyl ring with respect to metal-indenyl axis. A top view of the geometries in the optimum (13) and rotated conformations (14) are shown below. As a matter of convenience we changed the position of Mo(CO)$_2$(Allyl) unit instead of indenyl. Also we have pointed out previously the main interactions are between metal fragment 3a′, 1a″ and indenyl $3\pi_s$, $2\pi_a$ orbitals. 15 and 16 show interaction patterns and also the overlap integral between each fragment orbitals are listed. The overlap of the above dominant interactions is favored in the optimum, that is, the exo conformation.

Substituted Allyl complexes. A series of substituted allyl complexes have been studied with NMR method to assess the effect of steric hindrance in determining the conformational preferences of the allyl unit.[8] But only few struc-

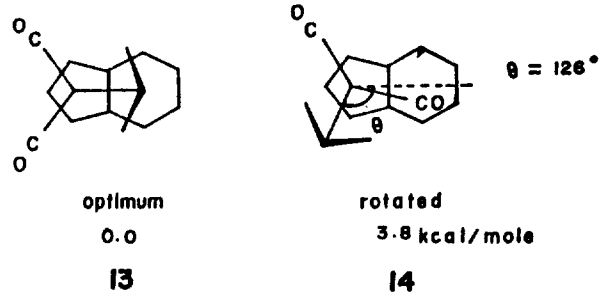

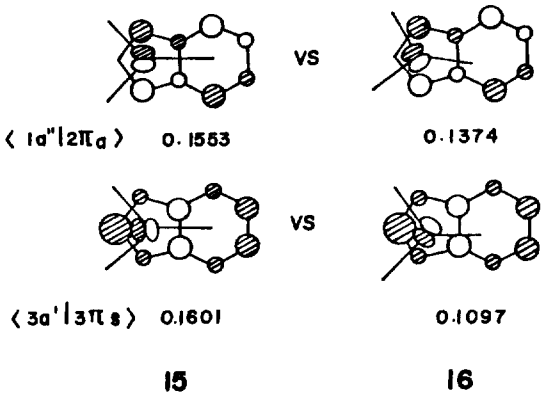

15 **16**

tural data are available.[2a),c),17] In general the allyl unit is part of a larger organic system. We optimized several substituted allyl complexes at the two limiting exo and endo orientations in (Allyl)Mo(CO)$_2$(Indenyl). Table 1 lists the each optimum geometry and relative energy to the exo conformation. The two variables, α and β, were also used as defined in 6. When methyl group is substituted at C_1 in syn position (see below the Table 1 for the numbering system) which is denoted as 1-s-Me, the optimum geometries are very close to those of unsubstituted allyl complex. And according to the relative energy, ΔE = 3.8 kcal/mol, which is almost identical to that of the unsubstituted allyl, the energy difference primarily comes from electronic effect, not from steric hindrance. However, the next complex, 1-a-Me, where methyl group is in anti-position, shows the different α values from above two allyl groups. In the exo anti-positioned methyl group sterically interacts with CO groups (see 17). In order to reduce this interactions α angle has been increased by 10 degree. In the endo the situation is different. The steric interaction of anti-methyl in the endo is with the indenyl ring. Therefore α angle has been reduced by amount of 5 degree. The steric effect on indenyl ring is bigger than that of the exo where steric force happens with CO groups. This fact can be observed at the calculated relative energy. ΔE in 1-a-Me allyl is 9.7 kcal/mol which is much larger difference than those of

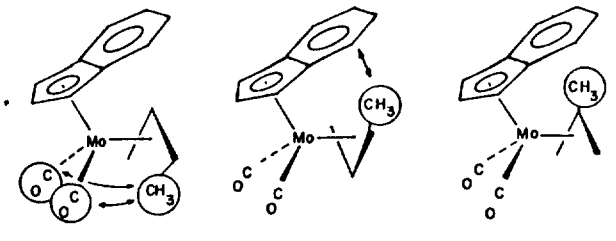

17

the above two. We also computed the total energy of 1-s-Me allyl exo complex is lower than that of 1-a-Me allyl by 14 kcal/mol. These results are corresponding to the experimentally observed in which the syn-orientation is thermodynamically more stable than the anti-orientation.[8] For 1,1-Me$_2$ allyl, computations give the very similar results to the 1-a-Me. Finally, the computational result of 2-substituted allyl, 2-Me, complex is very interesting. The optimum exo geometry shows very strong steric interaction between the 2-Me and indenyl ring (see 17). The α value is decreased to only 90°. However, the endo geometry is not affected by steric interaction as the optimized values are shown in Table 1. More interestingly, the endo is favorable over the exo geometry by 17.6 kcal/mol in total energy. In general the steric hindrance is important factor in substituted allyl indenyl complexes to determine the orientation of allyl moiety.

Table 2. Parameters Used in the Extended Hückel Calculations

Orbital	H_{ii}(eV)	ξ_1	ξ_2	C_1[a]	C_2[a]
Mo	4*d* -10.50	4.54	1.90	0.6097	0.6097
	5*s* -8.34	1.96			
	5*p* -5.24	1.90			
C	2*s* -21.40	1.625			
	2*p* -11.40	1.625			
H	1*s* -13.60	1.30			

[a]Contraction coefficients used in the double zeta expansion.

Acknowledgements. This research was supported by the Korean Science and Engineering Foundation.

Appendix

All calculations were performed using the extended Hückel method[18] with the modified Wolfsberg-Helmholz formula.[19] The parameters listed in Table 2 were taken from previous work.[20] All Mo-C(O), C-O, and C-H distances were set at 1.94, 1.14, and 1.09 Å, respectively. The Mo-polyene bond lengths were taken from experimental values of closely related compounds. All C-C (Allyl) and C-C (Indenyl) distances were idealized at 1.37 and 1.41Å. The C-Mo-C and C-C-C (Allyl) angles were kept at 90° and 120°, respectively. All substituents in allyl moiety were set to be bent 15° away from metal with respect to the allyl plane.

References

1. For reviews see (a) H. Yamamoto, H. Yasuda, K. Tatsumi, K. Lee, A. Nakamura, J. Chen, Y. Kai, and N. Kasai, *Organometallics*, **8**, 105 (1989); (b) R. D. Rogers, J. L. Atwood, T. A. Albright, W. A. Lee, and M. D. Rausch, *Organometallics*, **3**, 263 (1984); (c) L. M. Jackman and F. A. Cotton, Ed., "Dynamic Nuclear Magnetic Resonance Spectroscopy", Academic Press, New York, N. Y., 1975; (d) H. L. Clarke, *J. Organomet. Chem.*, **80**, 155 (1974).
2. (a) J. W. Faller, R. H. Crabtree, and A. Habib, *Organometallics*, **4**, 929 (1985); (b) A. S. Batsanov and Yu. T. Struchkov. *J. Organomet. Chem.*, **265**, 305 (1984); (c) J. W. Faller, H. H. Murray, D. L. White, and K. H. Chao, *Organometallics*, **2**, 400 (1983); (d) J. W. Faller, D. F. Chodosh, and K. Katahira, *J. Organomet. Chem.*, **187**, 227 (1980); (e) A. N. Nesmeyanov, N. A. Ustynyuk, L. G. Makarova, V. G. Andrianov, Yu. T. Struchkov, and S. Andrae, *J. Organomet. Chem.*, **159**, 189 (1978).
3. B. E. R. Schilling, R. Hoffmann, and D. L. Lichtenberger, *J. Am. Chem. Soc.*, **101**, 585 (1979).
4. T. A. Albright, J. K. Burdett, and M.-H. Whangbo, "Orbital Interactions in Chemistry", Wiley, New York, 1985.

5. B. E. R. Schilling, R. Hoffmann, and J. W. Faller, *J. Am. Chem. Soc.*, **101**, 592 (1979).
6. (a) M. L. H. Green, *Pure Appl. Chem.*, **50**, 27 (1978); (b) S. G. Davies, M. L. H. Green, and D. M. P. Mingos, *Nouveau J. Chim.*, **1**, 445 (1977).
7. R. S. Mulliken, *J. Chem. Phys.*, **23**, 1833, 1841, 2338, 2343 (1955).
8. J. W. Faller, C. C. Chen, M. J. Mattina, and A. Jakubowski, *J. Organomet. Chem.*, **52**, 361 (1973).
9. J. W. Faller and M. J. Incorvia, *Inorg. Chem.*, **7**, 840 (1968).
10. J. P. Collman, L. S. Hegedus, J. R. Norton, and R. G. Finke, "Principles and Applications of Organotransition Metal Chemistry", University Science Books, CA, 1987.
11. T. A. Albright, P. Hofmann, and R. Hoffmann, *J. Am. Chem. Soc.*, **99**, 7546 (1977) and references therein.
12. (a) A. J. Campbell, C. A. Fyfe, D. Harold-Smith, and K. R. Jeffrey, *Mol. Cryst. Liq. Cryst.*, **36**, 1 (1976); (b) F. van Meurs, J. M. vander Toorn, and H. van Bekkum, *J. Organomet. Chem.*, **113**, 341 (1976); (c) A. Eisenberg, A. Shaver, and T. Tsutsui, *J. Am. Chem. Soc.*, **102**, 1416 (1980).
13. R. D. Rogers, J. L. Atwood, T. A. Albright, W. A. Lee, and M. D. Rausch, *Organometallics*, **3**, 263 (1984).
14. (a) M. Mlekuz, P. Bougeard, B. G. Sayer, M. J. McGlinchey, C. A. Rodger, M. R. Churchill, J. W. Ziller, S. K. Kang, and T. A. Albright, *Organometallics*, **5**, 1656 (1986); (b) R. D. Barr, M. Green, T. B. Marder, and F. G. A. Stone, *J. Chem. Soc., Dalton Trans.*, 1261 (1984).
15. (a) R. Hoffmann, *Angew. Chem.*, **94**, 725 (1982); *Angew. Chem. Int. Ed.*, **21**, 711 (1982); (b) M. Elian, M. M. L. Chen, D. M. P. Mingos, and R. Hoffmann, *Inorg. Chem.*, **15**, 1148 (1976).
16. (a) P. Kubacek, R. Hoffmann, and Z. Havlas, *Organometallics*, **1**, 180 (1982); (b) R. Hoffmann, M. M. L. Chen, and D. L. Thorn, *Inorg. Chem.*, **16**, 503 (1977); (c) M. Elian and R. Hoffmann, *Inorg. Chem.*, **14**, 1058 (1975).
17. (a) G. Huttner, H. H. Brintzinger, L. G. Bell, P. Friedrich, V. Bejenke, and D. Neugebauer, *J. Organomet. Chem.*, **145**, 329 (1978); (b) F. A. Cotton and M. D. LaPrade, *J. Am. Chem. Soc.*, **90**, 5418 (1968).
18. R. Hoffmann, *J. Chem. Phys.*, **39**, 1397 (1963); R. Hoffmann and W. N. Lipscomb, *ibid*, **36**, 2179 (1962); **37**, 2872 (1962).
19. J. H. Ammeter, H. B. Bürgi, J. C. Thibeault, and R. Hoffmann, *J. Am. Chem. Soc.*, **100**, 3686 (1978).
20. R. H. Summerville and R. Hoffmann, *J. Am. Chem. Soc.*, **98**, 7240 (1976).

Asymmetric Synthesis of Both Enantiomers of 4-Hexanolide, a Component of the Female Sex Pheromone from the Dermestid Beetle *Trogoderma Glabrum*

Kwang-Youn Ko*

Korea Research Institute of Chemical Technology, Chungnam 305-306

E.L. Eliel

Department of Chemistry, University of North Carolina at Chapel Hill, Chapel Hill, NC, USA 27514.

Received September 4, 1989

Optically active (R)- and (S)-2-benzyloxy-1-butanol have been prepared by a previously described asymmetric synthesis based on a chiral oxathiane and have been converted into (R)-(+)-4-hexanolide, a component of the pheromone secreted by the female of the dermestid beetle, and its enantiomer.

Introduction

(R)-(+)-4-hexanolide (**1**) is a component of the pheromone secreted by the female of the demestid beetle *Trogoderma glabrum*.[1] The beetle has been reported to respond to the (R)-isomer but to neither the (S)-isomer nor the racemate.[1]

The preparation of optically active lactone **1** has received a great deal of synthetic attention, which may be categorized into three methods: 1) asymmetric reduction of suitable prochiral ketones with baker's yeast or chiral reducing agents,[2] 2) stereospecific synthesis from optically active starting materials such as glutamic acid[3a], D-(+)-ribolactone[3b], δ-D-(+)-gluconolactone[3c] and (R)-2,3-O-isopropylidene-D-glyceraldehyde[3d], 3) resolution of lactone precursors or lactones[4], and 4) other chiral methods such as Sharpless epoxidation[5a] or chiral sulfoxide methodology.[5b]

In the paper we report enantioselective syntheses of both enantiomers of 4-hexanolide, starting from 2-benzyloxy-1-butanol (**2**) which in turn, can be easily prepared based on chiral 1,3-oxathiane methodology.[6] As suggested in Scheme 1, the two-carbon homologation using malonate anion at the primary alcohol position followed by necessary manipulations of functional groups will lead to the product.